EXPANDING THE SCOPE OF CATALYTIC CARBON–HYDROGEN FUNCTIONALIZATION: SYNTHESIS OF MEDIICNALLY RELEVANT HETEROCYCLES

By

Melody Wu

A capstone project submitted for Graduation with University Honors

May 12, 2023

University Honors
University of California, Riverside

APPROVED

Dr. Kevin Kou
Department of Chemistry

Dr. Richard Cardullo, Howard H Hays Jr. Chair
University Honors

ABSTRACT

Heterocycles, cyclic organic molecules that contain nitrogen, oxygen, or sulfur, are functionally important fragments in pharmaceuticals and are found in 60% of FDA-approved drugs. These heterocycles can be synthesized via carbon–hydrogen (C–H) bond functionalization, an integral reaction in organic chemistry describing the direct breaking and transformation of normally unreactive C–H bonds. Conventional C–H functionalization involves reacting C–H bonds with electron-poor alkenes and alkynes; however, analogous reactivity with electron-rich substates is rare. This project aims to explore the novel mechanistic aspects of rhodium(III)-catalyzed C–H functionalization involving electron-rich alkenes to enable reactivity with new heterocyclic substrates under an oxygen-free environment. Furthermore, cobalt(III) metal is investigated as a more cost-effective and greener alternative to rhodium. The novel nature of this project represents potentially uncharted territories in studying new chemical space for medicinal chemistry.

ACKNOWLEDGEMENTS

First and foremost, I would like to thank my faculty mentor Dr. Kevin G.M. Kou for giving me the opportunity to grow as a researcher and an individual throughout my undergraduate career. His dedication to this project and to my journey in research, from extending advice during times of concern to providing me with opportunities to advance my science career, has deeply inspired and fostered my love for research. Thank you for believing in me and always encouraging me to do my best.

Within the Kou Research Lab, I would like to thank my graduate mentor, Yujie Cao, for her guidance and encouragement for the past two years. Her mentorship has allowed me to develop agency as a researcher and build a solid foundation in chemical research techniques and data analysis. I would also like to thank Andy Trinh for being incredibly supportive throughout the highs and lows of this project, and for always addressing my concerns and questions with patience. To the members of the Kou Research Lab, thank you for cultivating such a positive and inclusive work environment that has made my time here immensely enjoyable; I would not be where I am today without you all.

Lastly, I would like to thank the Chancellor's Research Fellowship and University Honors for funding this project. I would also like to thank the 2022-2023 cohort of Chancellor Research Fellows for their support in my research endeavors; their dedication and passion for their projects truly inspire me and I couldn't have asked for a better group of people to close off my undergraduate journey.

INTRODUCTION

Small molecule drugs have contributed significantly to the pharmaceutical industry and the medicinal chemistry space. Historically impactful drugs include Aspirin, registered in 1899 and Retrovir, registered in 1987. Still widely used today, aspirin is one of the first synthetic pharmaceutical drugs and provided an easily accessible way to relieve pain by inhibiting prostaglandin biosynthesis to decrease inflammation (Beck et. al., 2022). Retrovir is the first anti-HIV drug that started the efforts to turn a deadly infection into a manageable chronic condition (Beck et. al., 2022). The development of antiretroviral therapy has saved the lives of millions and continues to advance in capabilities. Out of all FDA-approved small-molecule drugs, 60% are nitrogen-containing heterocycles, building blocks common in medicinally relevant molecules (Vitaku et. al., 2014). Select examples of such pharmaceuticals include tipifarnib, which has anticancer properties, and primaquine, which is an antimalarial drug (*Figure 1*). These molecules are ubiquitous in natural products and pharmaceuticals due to their unique electronic and structural properties. Thus, new approaches to synthesizing heterocyclic compounds, especially those with new and underexplored chemical structures, are of great importance in the development of new pharmaceuticals.

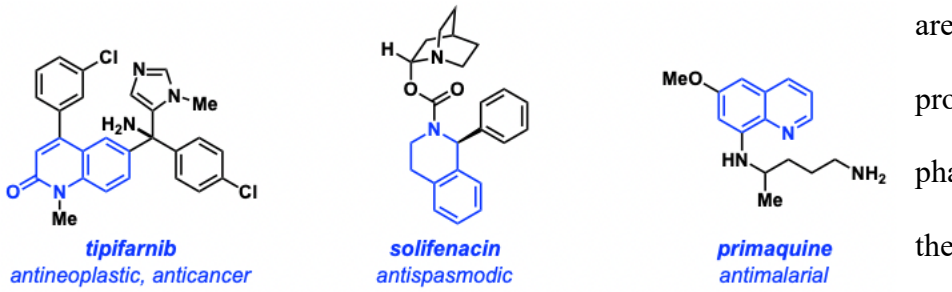

Figure 1. FDA-approved small-molecule pharmaceuticals containing nitrogen heterocycles.

The three most common types of naturally occurring and medicinally relevant molecules serving as the main building blocks of medicinally important molecules like Retrovir are terpenes,

alkaloids, and polyketides. This project specifically focuses on alkaloids, as they play an essential role in human medicine and the natural defenses of an organism, accounting for 20% of secondary metabolites in plants (Heinrich et. al., 2021). Alkaloids are compounds that contain at least one nitrogen in the molecule, and based on the structure, can be categorized into different classes such as pyrrolidines, pyridines, indoles, quinolines, and isoquinolones. Besides acting as building blocks for approved medicines like dopamine, serotonin, and drugs that contain penicillin, alkaloids are also present across a broad spectrum of categories. They are found in the spices (capsaicin) and coffee (caffeine) in our pantry, to toxins that have deeply impacted society, such as cocaine (Daley et. al, 2021). In 1804, German pharmacist Friedrich Sertürner isolated the first alkaloid, morphine, from the plant *Papaver somniferum*, more commonly known as the opium poppy (Kurek et. al., 2019). The discovery of morphine opened the doors for further investigation into isolating other types of alkaloids, such as berberine, which targets human bladder cancer, and papaverine, which displays antispasmodic properties (*Figure 2*). Due to its vast and diverse occurrence in plants, research devoted to alkaloid-based drugs became heavily emphasize. Today, there are at least 60 drugs approved worldwide that are plant-derived alkaloids (Daley et. al, 2021).

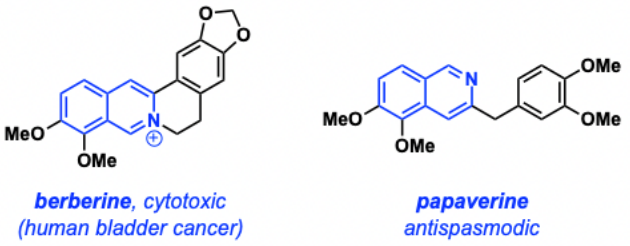

Figure 2. Examples of plant-derived alkaloids.

An important aspect to improving the performance of drugs derived from naturally occurring molecules, such as alkaloids, is to construct them synthetically and perform modifications. This is the strategy used to overcome obstacles such as antibiotic resistance. The biosynthesis of alkaloids, meaning how nature prepares them, involves amino acids such as lysine, histidine, tryptophan, and aspartic acid reacting with some form of a carbonyl precursor. Once the amino acids and the

carbonyl react, an iminium ion (a positive charge on the nitrogen) ensues. The last step of the biosynthesis undergoes a Mannich-like reaction to form the desired target. However, when synthesizing alkaloid-based small molecule drugs, combinatorial chemistry or multistep synthesis is necessary to achieve product formation. One such strategy is utilizing "click chemistry" reactions, highly favorable linking reactions where new groups are attached on carbo-heteroatom bonds (Hou et. al., 2012). These reactions are usually high yielding, easy to perform, and involve little to no purification (Kolb et. al, 2003). Some examples of click chemistry include cycloaddition reactions like Diels-Alder and nucleophilic ring opening of three-membered systems such as oxiranes, and these strategies have been utilized to form medicinally relevant molecules that have HIV protease inhibition properties (Brik et. al, 2003).

While there are various strategies to synthesize complex small, at the core, carbon–hydrogen (C–H) functionalization is one of the most integral yet simple reactions regarding small molecule synthesis. C–H functionalization describes the direct breaking and transformation of normally unreactive C–H bonds. It is a powerful reaction that opens doors for forming more complex molecules, including heterocycles, that are used in pharmaceutical and agricultural industries by leveraging bonds that would otherwise be inaccessible. Moreover, this reaction has the potential to be more atom-economical than the widely practiced, Nobel Prize-winning cross-coupling methods such as the Suzuki-Miyaura, the Negishi, and the Heck palladium-catalyzed cross coupling reactions (*Figure 3*) (Colby et. al., 2010). C–H functionalization replaces heavy halogens (*e.g.,* bromine and iodine) used in cross-coupling reactions, which act as a handle for chemical reactivity, with the lightest atom in the periodic table—hydrogen, thus minimizing the waste generated in the reactions by decreasing the weight of the byproduct. This reaction is often catalyzed by metals, and rhodium(III) is one of the most versatile despite its status as a precious

metal, due to its high compatibility with a wide array of molecules (*Figure 3*). Complementary to conventional C–H functionalization approaches involving Rh(III)/(I) catalysis that are typically confined to reactions with electron-deficient substrates, this project seeks to explore novel mechanistic aspects of said reaction using electron-rich substrates. The inspiration behind this project is based off

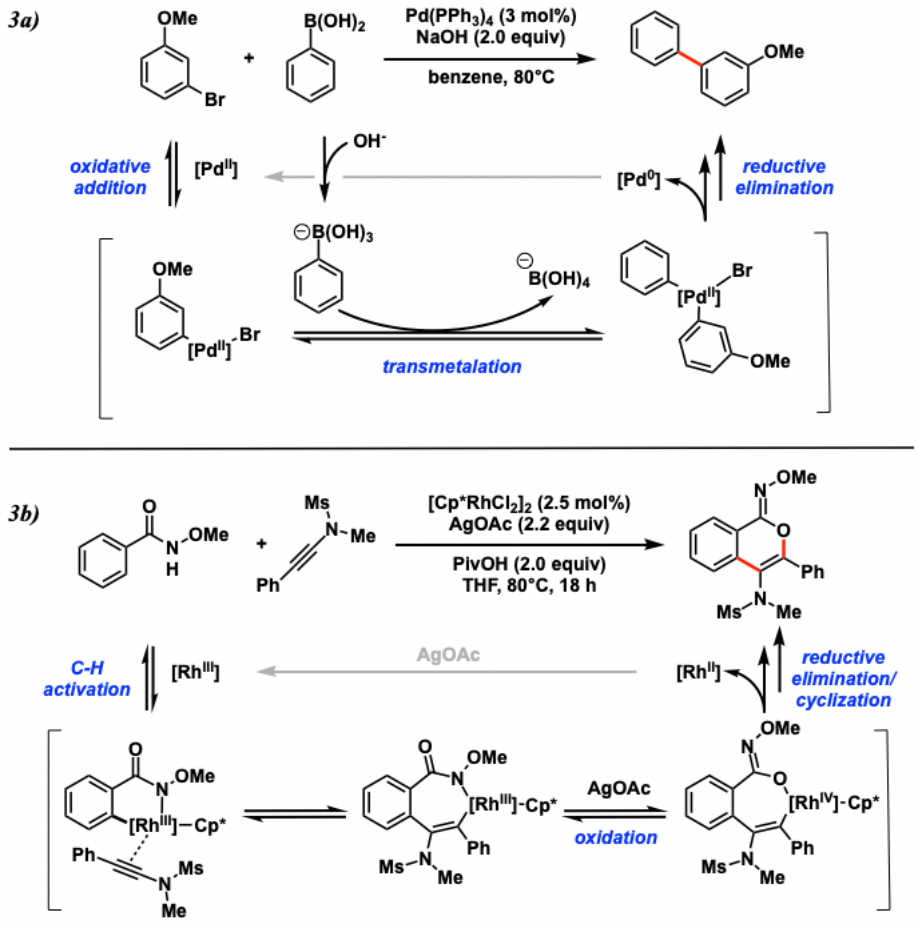

Figure 3. **a)** Pd-catalyzed cross-coupling vs. **b)** Rh-catalyzed C-H Functionalization

previous work from our group, the Kou Research lab, where we describe the first examples of the formation of isoquinolone molecules using electron-rich silyl enol ethers (Kou et. al., 2020). Synthesizing alkaloid-type molecules has been a common theme in our group, given these structures typically have a broad spectrum of activity and application. I plan to expand the scope of this process to include electron-rich alkynes, which we propose undergo typical Rh(III)/(I) catalytic cycle to form isoquinolone **3** and a distinctive Rh(III)/(IV)/(II) catalytic cycle to form oxime **4** (*Figure 4*).

Among current published literature, there are only a few examples of C–H functionalization reactions with electron-rich substrates to form isoquinolone-type structures, and even less with electron-rich alkynes. The Marsden group described a α-arylation of electron-rich vinyl esters with pivaloyl hydroxamate using rhodium(III) as a catalyst to yield an isoquinolone product (*Figure 4a*) (Webb et. al., 2014). Li and Wang were successful in constructing fluorinated heterocycles such as 4-fluoroisoquinolin-1(2*H*)-ones by reacting *N*-methoxy benzamide with 2,2-difluorovinyl tosylate (*Figure 4b*) (Wu et. al., 2017). However, the model alkene used in the study is substituted with electron-withdrawing fluorine groups to facilitate the migratory insertion process. Kakiuchi and coworkers reported the synthesis of α-aryl ketones from α-acylalkyl groups and cyclic alkenyl carbonates using rhodium-catalyzed C–H functionalization in 2015 (Hara et. al, 2015). The enol ester derivatives reported in the paper, like Li and Wang's work, are masked with electron-withdrawing groups in part to reduce electron density at the alkene. In 2018, the Wei group was successful

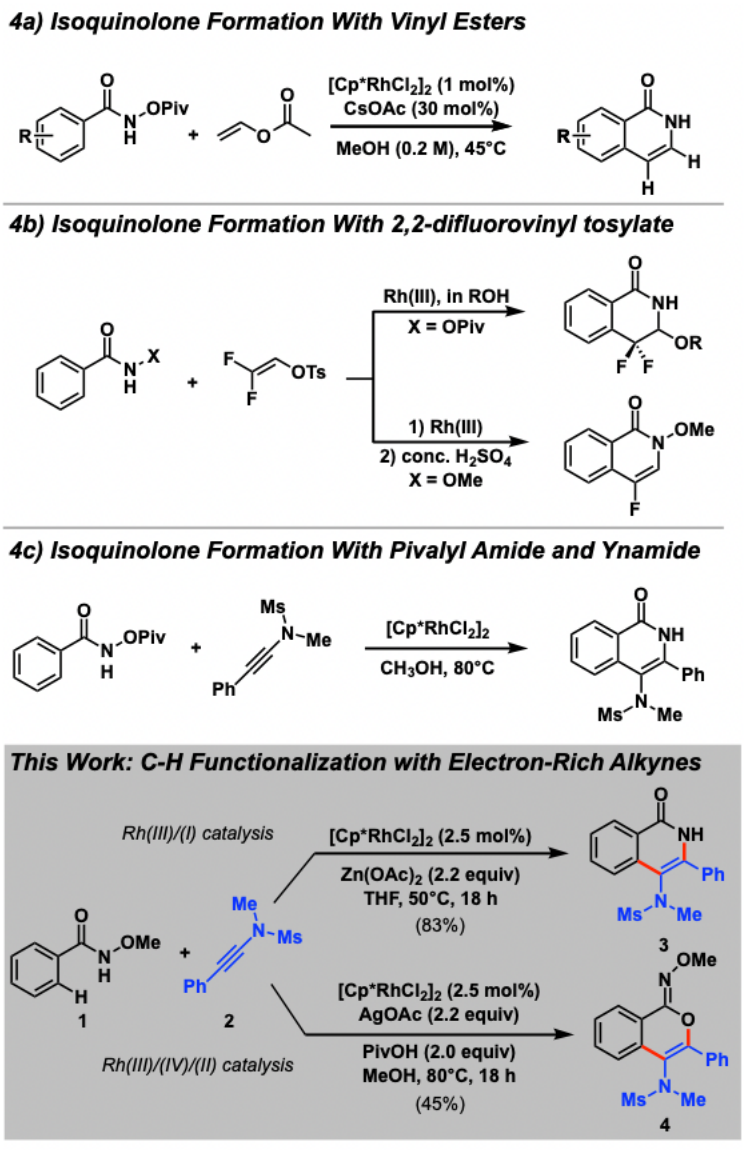

Figure 4 **.** Development of C-H Functionalization Reaction with Alkene and Alkyne Derivatives

in constructing isoquinolones from rhodium(III) catalyzed C–H functionalization of pivaloyloxy benzamide with ynamide **2** (*Figure 4c*) (Niu et. al., 2018). While success is demonstrated with current literature examples regarding rhodium catalyzed C–H functionalization with electron-rich substrates, most examples contain caveats that detract from such claims. Thus, C–H functionalization of electron-rich alkynes is rare, with the only successful example reported by the Wei group. In addition, the synthesis of isoquinolone molecules using rhodium in literature undergo the typical Rh(III)/(I) cycle; however, the formation of our oxime **4** isoquinolone is described to undergo the Rh(III)/(IV)/(II) cycle.

Herein, we report a chemodivergent strategy for the synthesis of isoquinolone **3** and oxime **4**, which to our knowledge, has not been reported. While isoquinolone **3** has been constructed previously by the Wei group using pivaloyloxy benzamide, this work focuses on the simpler (and thus more desirable) amide **1** and the underexplored electron-rich alkyne **2** as model substrates. In addition to this discovery, I also found that cobalt, an earth-abundant and cheaper metal residing in the same group as rhodium, displays similar reactivity. Cobalt's ability to form isoquinolone **3** hints at its potential as a promising alternative to rhodium catalysis. This capstone will expand our understanding of oxidative Rh(III) catalysis, which is far less studied compared to oxidative palladium and nickel catalyses. Further, using cobalt(III) for the C–H functionalization of electron-rich alkynes opens the possibility of a green-chemistry approach as well as the prospect of unprecedented oxidative cobalt-catalyzed C–H functionalization.

RESULTS AND DISCUSSION

*Reaction Condition Screening for Isoquinolone **3***

Initially, we investigated the role of additives in the process of constructing isoquinolone **3**. Amide **1** and the underexplored electron-rich alkyne **2** were selected as model substrates. Building on our previous project on heterocycle rearrangement, we conducted the reaction in THF at 50°C using 2.2 equivalences of silver acetate (AgOAc) as the additive and the rhodium(III) dimer $[Cp^*RhCl_2]_2$ as the catalyst. The reaction produced the desired product **3** in 31% yield (Table 1, entry 1). Despite the modest yield, we subsequently conducted the reaction using different additives to optimize the reaction conditions and examine their influence on the formation of isoquinolone **3**. When adjusting for equivalence of AgOAc the yield increased with increased equivalences of additive, however not significant enough (Table 1, entry 3). When performing the reaction with other silver-based additives produced poor yields, specifically silver nitrate ($AgNO_3$)

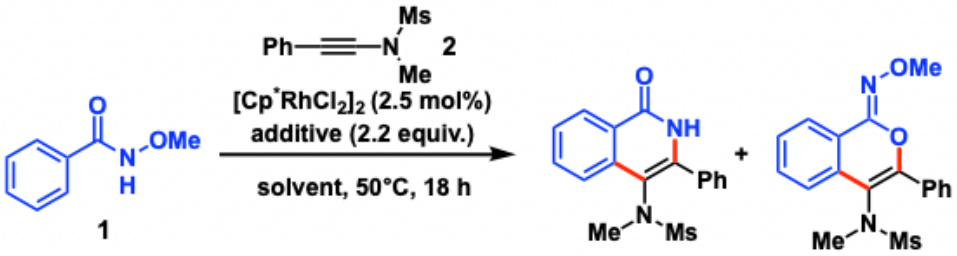

entry	additive	solvent	3	4
1	AgOAc	THF	31%	0%
2	AgOAc *(0.5 equiv)*	THF	19%	0%
3	AgOAc *(5.0 equiv)*	THF	35%	0%
4	$Cu(OAc)_2$	THF	4%	22%
5	$AgNO_3$	THF	4%	0%
6	Ag_2CO_3	THF	12%	0%
7	$Zn(OAc)_2$	THF	83%	0%
8	$Co(OAc)_2 \cdot 4H_2O$	THF	24%	0%
9	Cu(OAc)	THF	2%	9%
10	$Mn(OAc)_2$	THF	43%	0%
11	$Cu(OAc)_2$ *(2.0 equiv)* AgOAc *(0.2 equiv)*	Toluene	9%	25%
12	$Cu(OAc)_2$ *(2.0 equiv)* AgOAc *(0.2 equiv)*	1,4-dioxane	43%	18%
13	AgOAc	Methanol	0%	52%

Table 1. Optimization of the C-H Functionalization Reaction of Isoquinolone **3**.

and silver carbonate (Ag_2CO_3) (Table 1, entries 5-6). When $Mn(OAc)_2$ and $Co(OAc)_2•4H_2O$ were used as the additive, isoquinolone **3** was produced in 24% and 43% yield, respectively (Table 1, entries 10 and 8). When a combination of additives were used, the desired product was yielded in 43 % with 2 equivalences $Cu(OAc)_2$ and 0.2 equiv AgOAc; however, changes in solvent lead to drastic changes in yield (Table 1, entries 11-12). Using $Zn(OAc)_2$ saw a significant improvement of reaction yield of 83% (Table 1, entry 7). When copper-based additives were used such as copper(II) acetate and copper(I) acetate, we saw preference for the formation of oxime **4** over isoquinolone **3,** which has not been reported in the literature (Table 1, entries 4, 13). To further optimize the reaction conditions, various organic solvents, including toluene, 1,4-dioxane, and methanol, were screened. Under the same reaction conditions, using toluene gave higher selectivity for oxime **4** over isoquinolone **3** while using 1,4-dioxane yielded isoquinolone **3** in 43% (Table 1, entries 11-12). THF gave the best yields for isoquinolone **3**, as noted in entry 7 of Table 1. During solvent optimization, methanol was discovered to selectively yield oxime **4** (Table 1, entry 13).

Metal-Catalyzed C–H Functionalization with Enamides

After optimizing the conditions for isoquinolone **3**, the generality of C–H functionalization was explored using a second electron-rich substrate. The electron-rich alkyne **2** was modified to an electron-rich alkene **5**, which was used as the model substrate (Table 2). Two metal catalysts were tested, $[Cp^*RhCl_2]_2$ and a palladium catalyst $Pd(OAc)_2$ alongside additives that yielded product during the optimization of isoquinolone **3** (Table 2). In addition, a temperature study was conducted to test if increased temperature would facilitate the formation of the desired product. However, this substrate yielded trace amounts of product or no reaction despite extensive studies into additives, solvent, and temperature. We theorize that alkene **5** may be less reactive than alkyne **2** due to its lower propensity to bind to the metal catalyst.

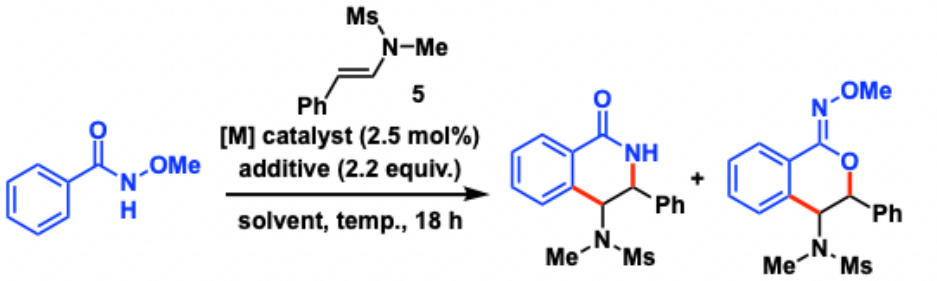

1 3 4

entry	metal catalyst	additive	solvent	temperature
1	$[Cp^*RhCl_2]_2$	AgOAc	THF	50°C
2	$[Cp^*RhCl_2]_2$	$Cu(OAc)_2$	THF	50°C
3	$[Cp^*RhCl_2]_2$	$Zn(OAc)_2$	THF	50°C
4	$[Cp^*RhCl_2]_2$	$Mn(OAc)_2$	THF	50°C
5	$[Cp^*RhCl_2]_2$	AgOAc	MeOH	50°C, 100°C
6	$[Cp^*RhCl_2]_2$	AgOAc	DCE	50°C, 100°C
7	$[Cp^*RhCl_2]_2$	AgOAc	TFE	100°C
8	$Pd(OAc)_2$	AgOAc	THF	50°C, 100°C
9	$Pd(OAc)_2$	AgOAc	DCE	50°C, 100°C
10	$Pd(OAc)_2$	$AgNO_3$	MeCN	100°C
11	$Pd(OAc)_2$	$AgSbF_6$	MeOH	100°C

Table 2. Reaction conditions tested with enamide **5**.

Reaction Condition Screening for Oxime 4

Motivated by the successful construction of isoquinolone **3**, we focused on the construction of novel oxime **4** using the same model substrates amide **1** and electron-rich alkyne **2**. We hypothesize that the formation of oxime **4** undergoes the oxidative Rh(III)/(IV)/(II) catalysis, where the rhodium(III) dimer is first activated by the silver acetate additive. Following that, the activated catalyst then attaches itself onto amide **1**. The complex then undergoes concerted metalation deprotonation, resulting in a five-membered intermediate with Rh(III) on the molecule. Ynamide **2** subsequently coordinates to the amide-rhodium complex and undergoes migratory insertion. This results in a seven-membered intermediate, which is oxidized by silver acetate to afford Rh(IV), which has preference for binding to oxygen over nitrogen in the catalytic cycle and is what favors

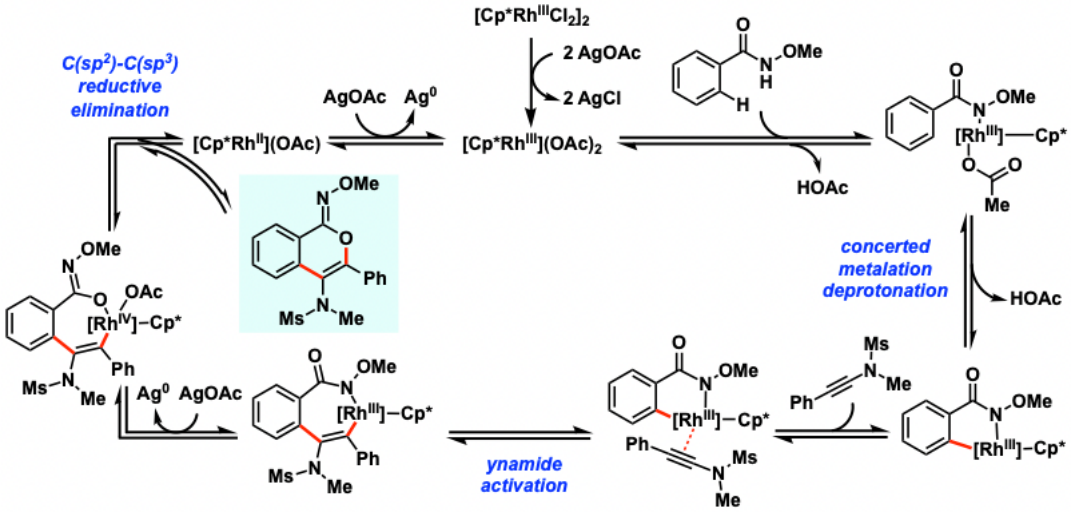

Figure 5. Rh(III)/(IV)/(II) Cycle Proposed Mechanism

formation of the oxime product. The metal complex undergoes reductive elimination to Rh(II), which leads to the formation of the said product. The silver acetate ligand on the Rh(II) is oxidized again to regenerate the rhodium(III) catalyst. The configuration of oxime **4** was confirmed by X-ray crystallographic analysis, ^{1}H nuclear magnetic resonance (NMR) spectra, and ^{13}C NMR spectra. As previously stated, oxime **4** has only been observed within a mixture of compounds when optimizing conditions for isoquinolone **3.** While cyclic oximes of this type have been

produced prior, they have only appeared as side products, and developing a reliable method to synthesize them fills a gap in the chemical literature while also uncovering new oxidation-enabled Rh(III)/I(IV)/(II) catalysis (*Figure 5*) (Guimond et. al., 2010).

The C–H functionalization of amide **1** and alkyne **2** to oxime **4** was investigated based on entry 13 in Table 1, where selectivity for oxime is observed. This reaction, using $[Cp^*RhCl_2]_2$ as the catalyst, AgOAc as the additive with methanol at 50°C yielded oxime **4** in 52%. We proceeded to adjust for different catalysts, additives, temperatures, and organic solvents to optimize the reaction

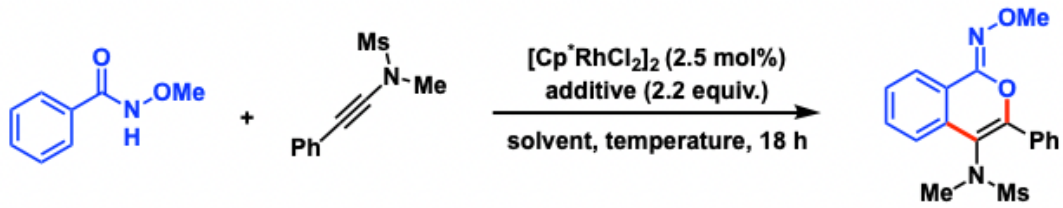

entry	metal catalyst	additive	solvent	temperature	yield
1	$[Cp^*RhCl_2]_2$	AgOAc	MeOH	50°C	52%**
2	$[Cp^*RhCl_2]_2$	AgOAc	MeOH	25°C	15%**; 60%** [d]
3	$[Cp^*RhCl_2]_2$	AgOAc [a] $FeCl_3$	MeOH	50°C	n/a
4	$[Cp^*RhCl_2]_2$	AgOAc [a] $FeCl_3$	Toluene	50°C	n/a
5	$[Cp^*RhCl_2]_2$	AgOAc AcOH	MeOH	80°C	37%*; 60%** [e]
6	$[Cp^*RhCl_2]_2$	AgOAc PivOH	MeOH	80°C	48%*
7	$Cp^*Co(CO)I_2$	CsOAc [b] $AgSbF_6$	TFE	100°C	39% [f]
8	$Cp^*Co(CO)I_2$	CsOAc [b] $AgSbF_6$ PivOH	TFE	100°C	27% [f]
9	$[Cp^*RhCl_2]_2$	AgOAc [c] $FeCl_3$	THF	100°C	n/a
10	$[Cp^*RhCl_2]_2$	AgOAc	IPA	50°C	11% [f]
11	$[Cp^*RhCl_2]_2$	AgOAc	EtOH	50°C	27% [f]

Table 3. Optimization of the C-H Functionalization Reaction of Oxime **4**. [a]AgOAc (0.2 eq), $FeCl_3$ (2.0 eq).[b]CsOAc (1.0 eq), $AgSbF_6$ (0.2 eq). [c]AgOAc (6.7 eq), $FeCl_3$ (2.2 eq). [d] 60% amide **1** S.M. [e] 37% isolated yield of oxime; NMR yield 6% amide **1** S.M. **4**. [f] Isoquinolone **3** yield. *Not completely clean, still purifying. **NMR yields with 1,3,5-trimethylbenzene as internal standard.

conditions and examine how such conditions affected the construction of oxime **4**. When adjusting for equivalence of AgOAc, 2.2 equivalence gave the best results, and using a mixture of AgOAc and $FeCl_3$ yielded no reaction (Table 3, entries 3-4). The addition of either pivalic acid or acetic acid was also examined, and we observed that 2 equivalences of pivalic acid gave slightly cleaner spectra compared to acetic acid; however, the yields were similar with 48% isolated desired oxime for pivalic acid and 37% isolated desired oxime for acetic acid. To further optimize the reaction conditions, various solvents including toluene, ethanol, THF, IPA, TFE, and methanol were screened. THF and toluene did not result in any product **4** formed (Table 3, entries 4, 9), while IPA, TFE, and ethanol gave isoquinolone **3** in low yields (Table 3, entries 7, 10, 11). Reactions conducted with methanol gave the highest yields. A temperature study was also conducted. With 50°C, yields were moderate, with entry 1 of Table 3 giving the highest yield. When temperature was lowered to 25°C, there was a drastic drop in yield (Table 3, entry 2). Increasing the temperature to 80°C yielded the highest oxime formation with the least amount of starting material; based on NMR analysis of the reaction mixture, we observed 60% oxime formation and 6% starting material (Table 3, entry 5). The starting material recovery increases when the temperature is over 80°C, specifically when the reaction is conducted at 100°C.

*Amide Substrate Scope of Oxime **4***

Next, the scope of amide **1** containing various R groups was investigated (*Figure 3*). Para-substituted halogens on the phenyl ring yield the corresponding oxime in varying yields, with para-substituted fluorine **4b** at 23% and bromine **4c** at 11% (*Figure 3*). When the phenyl ring contains a para-substituted acetoxy group **4a**, the oxime product is produced in 24% (*Figure 3*). If the R group is in the meta position of the ring, it yields the oxime product in 29% when the R group is chlorine **4f** and only yields isoquinolone if the R group is a methyl group **4e**. Replacing the 6-

membered ring of amide **1** with a furan also produces oxime **4d** but in low yields (*Figure 6*). This portion of the project is still on-going, and I aim to increase the isolated yields.

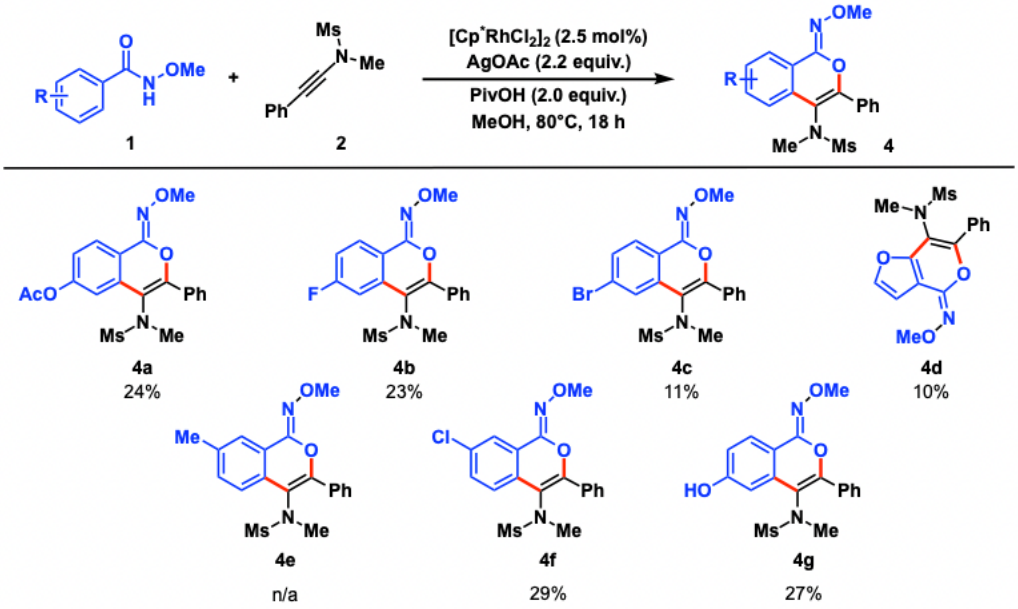

Figure 6. Current Substrate Scope of C-H Functionalization Reaction of Oxime **4**

Alternatives to Rhodium-Catalyzed C–H Functionalization

When optimizing the reaction conditions to synthesize oxime **4**, a cobalt(III) catalyst was used instead of the rhodium dimer $[Cp^*RhCl_2]_2$ to test for alternatives to rhodium catalysis, as achieving similar results with earth-abundant and cheaper metals is desirable. Using $Cp^*Co(CO)I_2$ as the catalyst, cesium acetate CsOAc with $AgSbF_6$ as the additive in TFE, the formation of isoquinolone **3** was observed in 46%. A regioisomer of isoquinolone **3** was also observed at 38% yield, where the phenyl group and the amine group switch positions. While the formation of oxime **4** was not observed, the current obtained results are still promising as typically, cobalt-catalyzed C–H functionalization reactions require complex directing groups. Li and coworkers[9a] describe the formation of quinazoline products using cobalt-catalyzed C–H functionalization using arenes such as *N*-sulfinylimines with dioxazolones as a directing group to facilitate the reaction (*Figure 7a*) (Wang et. al., 2016). In 2019, Niu and Song were successful in using complex heterocycles such

as α-imino-oxy acid with a *N,O*-bidentate directing group to access isoquinolones (*Figure 7b*) (Li et. al, 2019). Using electrochemistry, Dong and Huang were able to synthesize complex dihydroisoquinolone derivatives from benzamides containing quinone moieties and alkenes (*Figure 7c*) (Huang et. al., 2022). In the literature mentioned, the benzamide substrates used are very complex and usually have bulky directing groups; however, we were successful in forming isoquinolone **3** with simple substrates and these results encouraged us to further investigate this route (*Figure 7*). Additionally, while there are examples of cobalt(III) reaction with simpler amides, none feature the alkoxyamides used in this project (Banjare et. al., 2021). Currently, other lab members within the group, namely Yujie Cao, Andy Trinh, and Shayne Cruz, are pursuing this route.

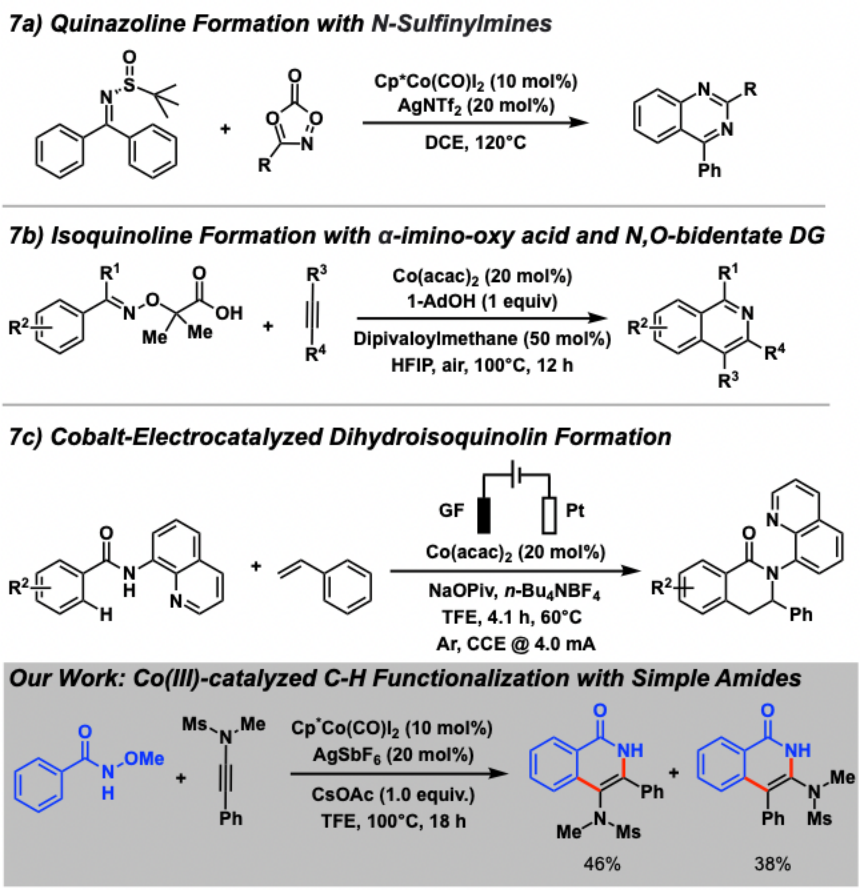

Figure 7. Development of Co-catalyzed C-H Functionalization with Various Complex Directing Groups vs. Our Simple Methoxyamide Substrate

CONCLUSIONS AND FUTURE WORK

In summary, we have optimized reaction conditions for the formation of amino-substituted isoquinolone product **3**. This approach was extended to developing new catalysis methodologies to form novel oxime 4. These results have allowed us to have a better mechanistic understanding

of C–H functionalization chemistry enabled by group IX metals, while generating amino-substituted isoquinolone products and novel cyclic oxime. Moving forward, our group will continue further studying the C–H functionalization reaction with electron-rich substrates, including continued exploration of the amide and ynamide substrate scope for the oxime molecule. Currently, we are working on constructing new ynamides to test in our oxime condition (*Figure 8a*). In addition, group members Andy Trinh and Shayne Cruz will be developing the cobalt catalysis aspect of the project with electrochemistry (*Figure 8b*).

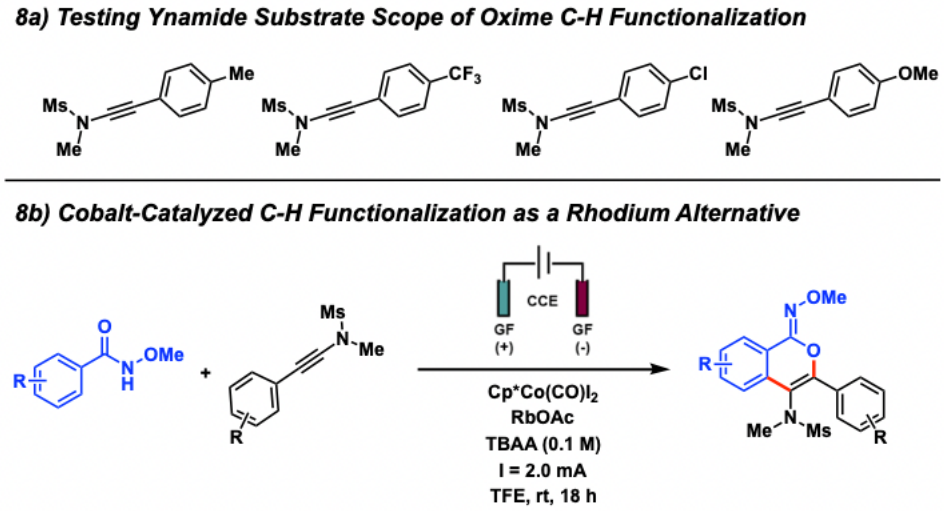

Figure 8. Future Work on C-H Functionalization in the Kou Research Lab.

EXPERIMENTAL SECTION

a. Formation of Amide **1**

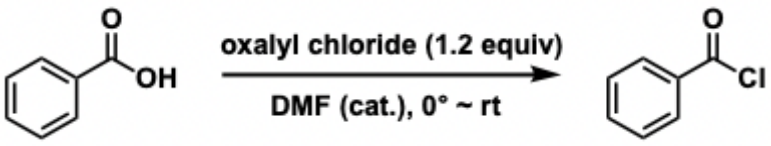

1) To a solution of the carboxylic acid (10mmol, 1.0 equiv) in dry CH_2Cl_2 (133 mL) at 0°C under N_2 was added dropwise oxalyl chloride (1.03 mL, 12 mmol, 1.2 equiv) followed by a catalytic amount of dry DMF (3 drops). The reaction was allowed to stir at room temperature until completion, typically 4 hours. The solvent was then removed under reduce pressure to afford the corresponding crude acid chloride.

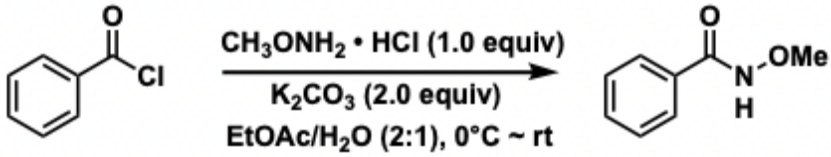

2) *O*-Methylhydroxylamine hydrochloride (4.17 mL used, 35.92 mmol, 1.0 equiv) was added to a biphasic mixture of K_2CO_3 (9.9286 g used, 71.84 mmol, 2.0 equiv) in a 2:1 mixture of EtOAc (240 mL used, 0.1 M equiv) and H_2O (120 mL used, 0.1 M equiv). The resulting solution was cooled to 0 degree followed by dropwise addition of the benzoyl chloride (4.17 mL used, 35.92 mmol, 1.0 equiv). The reaction was allowed to stir overnight while gradually allowing to warm to rt. Afterwards, the phases were separated, and the aqueous phase was extracted three times with EtOAc. The combined organic layers were dried over $NaSO_4$, filtered, and evaporated under reduced pressure. The pure products were obtained without any further purification or purification by column chromatography. ^{1}H NMR (500 MHz, $CDCl_3$) δ 7.77 – 7.71 (d, 2H), 7.55 – 7.50 (t, 1H), 7.44 (d, 2H), 3.89 (s, 3H).

b. Formation of Ynamide ***2***

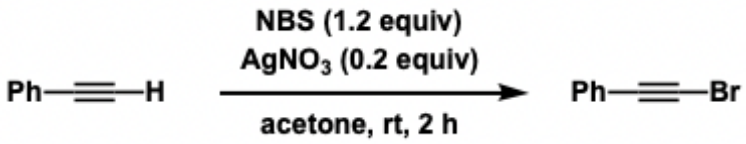

1) To a solution of the alkyne (1 equiv, 30 mmol) in anhydrous acetone (conc = 0.30 M, 17 mL) were added *N*-bromosuccinimide (1.2 equiv, 36 mmol) and $AgNO_3$ (10 mol%, 3.0 mmol). After 1 h at room temperature, the same quantity of $AgNO_3$ (10 mol%, 3.0 mmol) was added and the mixture was stirred at room temperature for 1 h. The resulting mixture was then filtrated, and then filtrate was extracted with hexane or CH_2Cl_2 (3 x 20 mL) The combined organic layers were washed with a 10% aqueous solution of HCl (2x 30 mL), brine (30 mL), dried (Na_2SO_4) and concentrated under vacuum (25°C, 15 mbar). The desired compound was obtained after purification by column chromatography (hexanes 100%). *This reaction is carried out away from light.*

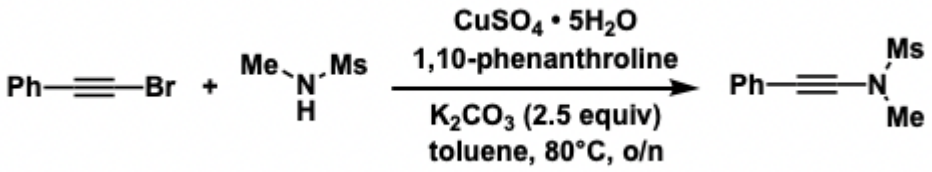

2) To a dried flask was added *N*-methylmethanesulfonamide (1.2 equiv, 29.64 mmol), $CuSO_4$ (0.1 equiv, 2.47 mmol), H_2O (0.5 equiv, 12.35 mmol), 1,10-phenanthroline (0.2 equiv, 4.94 mmol) and K_2CO_3 (2.5 equiv, 61.75 mmol), and this mixture was subsequently treated with anhydrous toluene (3 mL) and bromoalkyne (1 equiv, 24.7 mmol). The flask was purged with nitrogen gas, and then solution was heated at 80°C overnight. After completion, the crude reaction mixture was cooled to room temperature, filtered through Celite™, and concentrated *in vacuo*. Purification of the crude residue using silica gel flash column chromatography (hexanes:EtOAc, 4:1) gave

the pure ynamide as a pale-yellow oil (2.89 g, 56%). ^{1}H NMR (500 MHz, $CDCl_3$) δ 7.44 – 7.38 (m, 2H), 7.31 (m, *J* = 2.9 Hz, 3H), 3.30 (s, 3H), 3.13 (s, 3H).

c. *Formation of enamide* ***5***

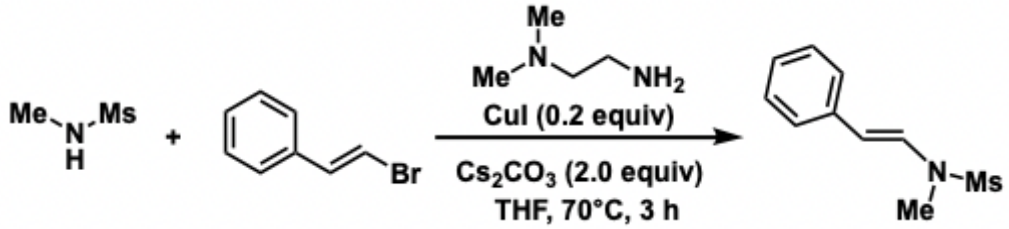

Copper iodide (95.2 mg, 0.5 mmol, 0.2 equiv), cesium carbonate (1.63 g, 5.0 mmol, 2.0 equiv.) and *N*-methyl-*N*-methanesulfonamide (0.229 mL, 2.5 mmol, 1 equiv) were successively added to a Schlenk tube and then purged by three successive vacuum-argon cycles. THF (7.58 mL) was then added, followed by *N,N'*-dimethylethylenediamine (0.108 mL, 1.0 mmol, 0.4 equiv) and β-bromostyrene (0.353 mL, 2.75 mmol, 1.1 equiv). After 3 h at reflux the mixture was cooled to room temperature, diluted with ethyl acetate, and filtered over silica. After concentration under reduced pressure the crude enamide was purified by flash column chromatography on silica gel (DCM 100%) to give the desired enamide as an amorphous powder (435.1 mg, 82.4%). ^{1}H NMR (600 MHz, $CDCl_3$) δ 7.36 (d, *J* = 14.4, 1H), 7.32 – 7.29 (m, 4H), 5.83 (d, *J* = 14.4 Hz, 1H), 3.19 (s, 3H), 2.91 (s, 3H).

d. *Formation of isoquinolone* ***3***

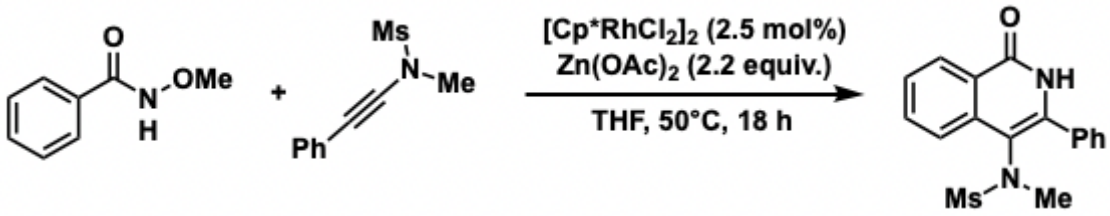

In a nitrogen-filled glove box, a 4 mL vial equipped with a magnetic stirring bar was charged with amide **1** (15.1 mg, 0.1 mmol, 1 equiv), ynamide **2** (25.1 mg, 0.12 mmol, 1.2

equiv), $[Cp^*RhCl_2]_2$ (1.5 mg, 0.0025 mmol, 0.025 equiv), and $Zn(OAc)_2$ (40.4 mg, 0.22 mmol, 2.2 equiv). Anhydrous THF (1.0 mL) was then added to the vial via syringe. The vial was sealed with a septum cap and removed from the glove box. The reaction mixture was heated at 50 °C for 18 h, then filtered over silica. After concentration under reduced pressure, the crude mixture was purified via preparatory thin-layer chromatography (hexanes:acetone, 1:1) to obtain the desired product (27.2 mg, 83%). ^{1}H NMR (500 MHz, $CDCl_3$) δ 9.79 (s, 1H), 8.33 (d, *J* = 8.0 Hz, 1H), 7.80 (d, *J* = 3.7 Hz, 2H), 7.57 – 7.51 (m, 6H), 3.30 (s, 3H), 2.24 (s, 3H).

*e. Formation of oxime **4***

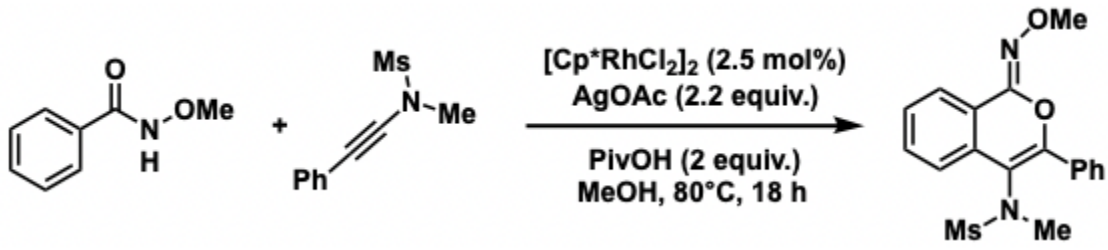

To a 4 mL vial equipped with a magnetic stirring bar was added pivalic acid (20.4 mg, 0.2 mmol, 2 equiv). The vial was then moved into a nitrogen-filled glove box, where it was charged with amide **1** (15.1 mg, 0.1 mmol, 1 equiv), ynamide **2** (25.1 mg, 0.12 mmol, 1.2 equiv), $[Cp^*RhCl_2]_2$ (1.5 mg, 0.0025 mmol, 0.025 equiv), and AgOAc (36.7 mg, 0.22 mmol, 2.2 equiv). Anhydrous MeOH (1.0 mL) was then added to the vial via syringe. The vial was sealed with a septum cap and removed from the glove box. The reaction mixture was heated at 80 °C for 18 h, then filtered over silica. After concentration under reduced pressure, the crude mixture was purified via preparatory thin-layer chromatography (hexanes:acetone, 1:1). A second preparatory TLC purification (CH_2Cl_2:methanol 95:5) was performed to obtain the desired product (20.3 mg, 65%). ^{1}H NMR (500 MHz, $CDCl_3$)

δ 7.99 (d, *J* = 8.0 Hz, 1H), 7.65 (d, *J* = 7.1 Hz, 2H), 7.50 (m, *J* = 21.2, 7.5 Hz, 5H), 7.36 (t, *J* = 7.6 Hz, 1H), 3.95 (s, 3H), 3.30 (s, 3H), 2.28 (d, 3H).

f. Formation of oxime ***4a***

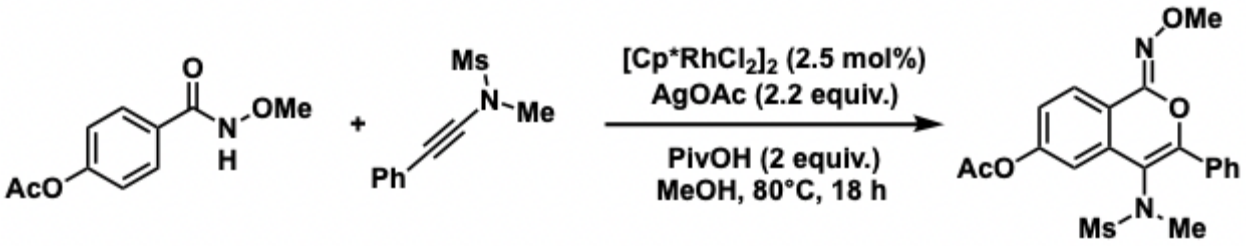

To a 4 mL vial equipped with a magnetic stirring bar was added pivalic acid (20.4 mg, 0.2 mmol, 2 equiv). The vial was then moved into a nitrogen-filled glove box, where it was charged with 4-(methoxycarbanoyl)phenyl acetate (20.9 mg, 0.1 mmol, 1 equiv), ynamide **2** (25.1 mg, 0.12 mmol, 1.2 equiv), $[Cp^*RhCl_2]_2$ (1.5 mg, 0.0025 mmol, 0.025 equiv), and AgOAc (36.7 mg, 0.22 mmol, 2.2 equiv). Anhydrous MeOH (1.0 mL) was then added to the vial via syringe. The vial was sealed with a septum cap and removed from the glove box. The reaction mixture was heated at 80 °C for 18 h, then filtered over silica. After concentration under reduced pressure, the crude mixture was purified via preparatory thin-layer chromatography (hexanes:acetone, 1:1). ^{1}H NMR (600 MHz, $CDCl_3$) δ 8.00 (d, *J* = 8.6 Hz, 1H), 7.68 – 7.63 (m, 2H), 7.52 – 7.44 (m, 5H), 3.94 (s, 3H), 3.28 (s, 3H), 2.33 (s, 3H), 2.29 (s, 3H).

g. Formation of oxime ***4b***

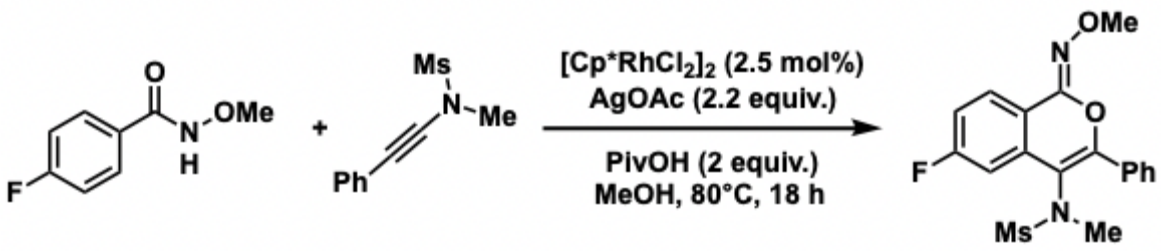

To a 4 mL vial equipped with a magnetic stirring bar was added pivalic acid (20.4 mg, 0.2 mmol, 2 equiv). The vial was then moved into a nitrogen-filled glove box, where it was charged with 4-fluoro-*N*-methoxybenzamide (16.9 mg, 0.1 mmol, 1 equiv), ynamide **2** (25.1 mg, 0.12 mmol, 1.2 equiv), $[Cp^*RhCl_2]_2$ (1.5 mg, 0.0025 mmol, 0.025 equiv), and AgOAc (36.7 mg, 0.22 mmol, 2.2 equiv). Anhydrous MeOH (1.0 mL) was then added to the vial via syringe. The vial was sealed with a septum cap and removed from the glove box. The reaction mixture was heated at 80 °C for 18 h, then filtered over silica. After concentration under reduced pressure, the crude mixture was purified via preparatory thin-layer chromatography (hexanes:acetone, 1:1). ^{1}H NMR (600 MHz, $CDCl_3$) δ 7.98 (d, J = 8.8, 1H), 7.67 – 7.62 (m, 2H), 7.52 – 7.45 (m, 5H), 3.93 (s, 3H), 3.28 (s, 3H), 2.28 (s, 3H).

h. Formation of oxime ***4c***

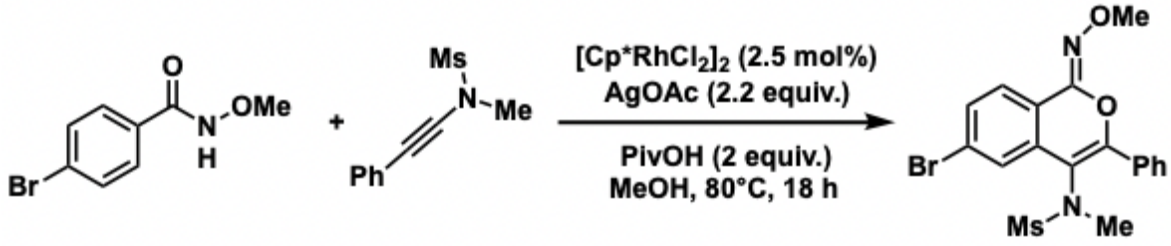

To a 4 mL vial equipped with a magnetic stirring bar was added pivalic acid (20.4 mg, 0.2 mmol, 2 equiv). The vial was then moved into a nitrogen-filled glove box, where it was charged with 4-bromo-*N*-methoxybenzamide (23.0 mg, 0.1 mmol, 1 equiv), ynamide **2** (25.1 mg, 0.12 mmol, 1.2 equiv), $[Cp^*RhCl_2]_2$ (1.5 mg, 0.0025 mmol, 0.025 equiv), and AgOAc (36.7 mg, 0.22 mmol, 2.2 equiv). Anhydrous MeOH (1.0 mL) was then added to the vial via syringe. The vial was sealed with a septum cap and removed from the glove box. The reaction mixture was heated at 80 °C for 18 h, then filtered over silica. After concentration under reduced pressure, the crude mixture was purified via preparatory thin-

layer chromatography (hexanes:acetone, 7:3). ^{1}H NMR (500 MHz, $CDCl_3$) δ 7.84 (d, J = 8.4 Hz, 1H), 7.66 – 7.60 (m, 2H), 7.47 (m, 5H), 3.94 (s, 3H), 3.29 (s, 3H).

*i. Formation of oxime **4d***

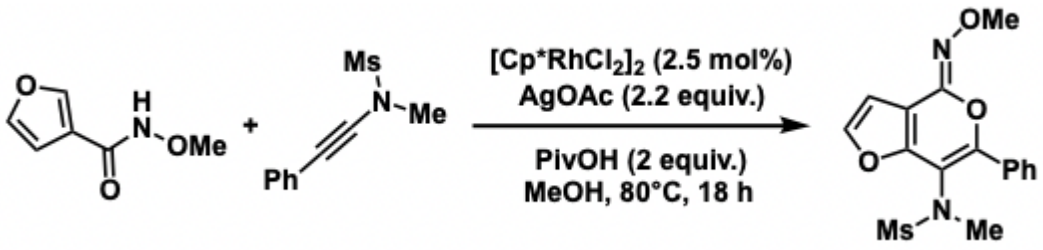

To a 4 mL vial equipped with a magnetic stirring bar was added pivalic acid (20.4 mg, 0.2 mmol, 2 equiv). The vial was then moved into a nitrogen-filled glove box, where it was charged with *N*-methoxyfuran-3-carboxamide (14.1 mg, 0.1 mmol, 1 equiv), ynamide **2** (25.1 mg, 0.12 mmol, 1.2 equiv), $[Cp^*RhCl_2]_2$ (1.5 mg, 0.0025 mmol, 0.025 equiv), and AgOAc (36.7 mg, 0.22 mmol, 2.2 equiv). Anhydrous MeOH (1.0 mL) was then added to the vial via syringe. The vial was sealed with a septum cap and removed from the glove box. The reaction mixture was heated at 80 °C for 18 h, then filtered over silica. After concentration under reduced pressure, the crude mixture was purified via preparatory thin-layer chromatography (hexanes:acetone, 1:1). A second and third preparatory TLC (hexanes:acetone 7:3) was run for purification. ^{1}H NMR (500 MHz, $CDCl_3$) δ 7.52 (m, 3H), 7.50 – 7.42 (m, 3H), 7.11 (d, J = 2.1 Hz, 1H), 4.25 (s, 3H), 3.26 (s, 3H), 2.19 (s, 3H).

*j. Formation of oxime **4f***

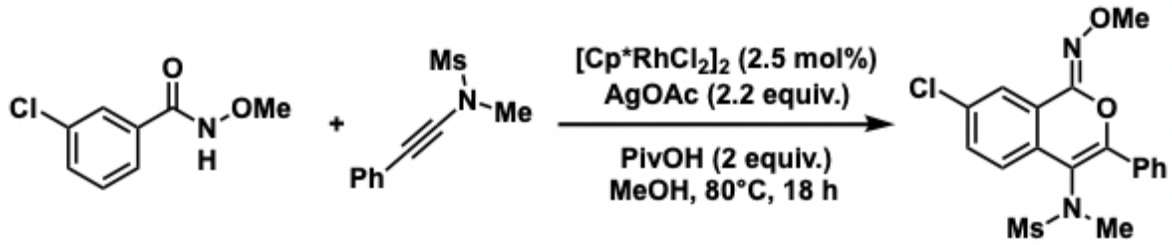

To a 4 mL vial equipped with a magnetic stirring bar was added pivalic acid (20.4 mg, 0.2 mmol, 2 equiv). The vial was then moved into a nitrogen-filled glove box, where it was charged with 3-chloro-*N*-methoxybenzamide (18.6 mg, 0.1 mmol, 1 equiv), ynamide **2** (25.1 mg, 0.12 mmol, 1.2 equiv), $[Cp^*RhCl_2]_2$ (1.5 mg, 0.0025 mmol, 0.025 equiv), and AgOAc (36.7 mg, 0.22 mmol, 2.2 equiv). Anhydrous MeOH (1.0 mL) was then added to the vial via syringe. The vial was sealed with a septum cap and removed from the glove box. The reaction mixture was heated at 80 °C for 18 h, then filtered over silica. After concentration under reduced pressure, the crude mixture was purified via preparatory thin-layer chromatography (hexanes:acetone, 7:3). A second and third preparatory TLC (CH_2Cl_2:methanol 98:2) was run for purification. ^{1}H NMR (500 MHz, $CDCl_3$) δ 7.97 (d, *J* = 2.1 Hz, 1H), 7.66 – 7.61 (m, 2H), 7.51 – 7.45 (m, 4H), 7.39 (d, *J* = 8.5 Hz, 1H), 3.95 (s, 3H), 3.27 (s, 3H), 2.27 (s, 3H).

*k. Formation of oxime **4g***

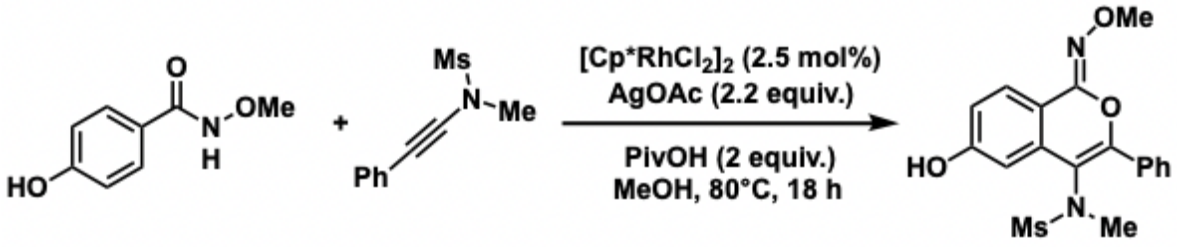

To a 4 mL vial equipped with a magnetic stirring bar was added pivalic acid (20.4 mg, 0.2 mmol, 2 equiv). The vial was then moved into a nitrogen-filled glove box, where it was charged with 4-hydroxy-*N*-methoxybenzamide (16.7 mg, 0.1 mmol, 1 equiv), ynamide **2** (25.1 mg, 0.12 mmol, 1.2 equiv), $[Cp^*RhCl_2]_2$ (1.5 mg, 0.0025 mmol, 0.025 equiv), and AgOAc (36.7 mg, 0.22 mmol, 2.2 equiv). Anhydrous MeOH (1.0 mL) was then added to the vial via syringe. The vial was sealed with a septum cap and removed from the glove

box. The reaction mixture was heated at 80 °C for 18 h, then filtered over silica. After concentration under reduced pressure, the crude mixture was purified via preparatory thin-layer chromatography (hexanes:acetone, 7:3). ^{1}H NMR (500 MHz, $CDCl_3$) δ 7.87 (d, *J* = 8.6 Hz, 1H), 7.62 (dd, *J* = 7.2, 2.4 Hz, 2H), 7.50 – 7.44 (m, 3H), 6.88 (d, *J* = 2.4 Hz, 1H), 6.84 (d, 1H), 3.92 (s, 3H), 3.25 (s, 3H), 2.28 (s, 3H).

^{1}H NMR SPECTRA

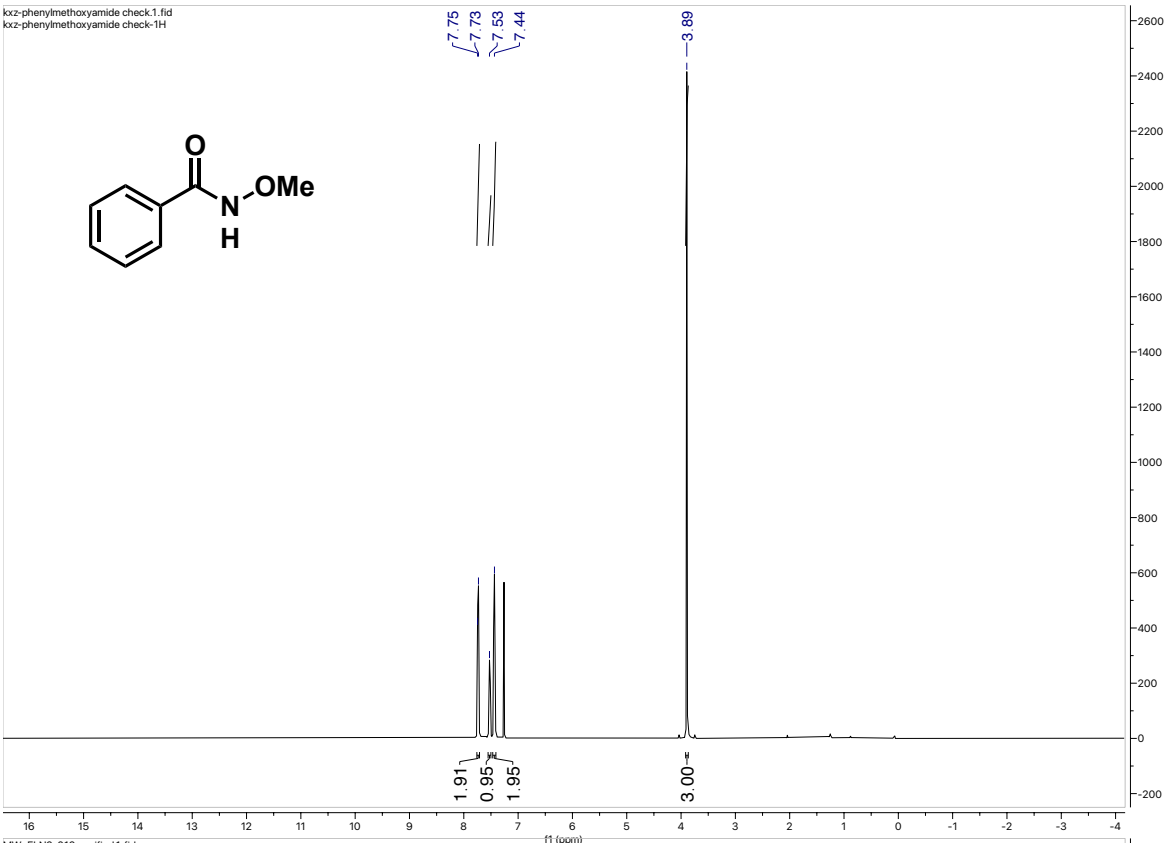

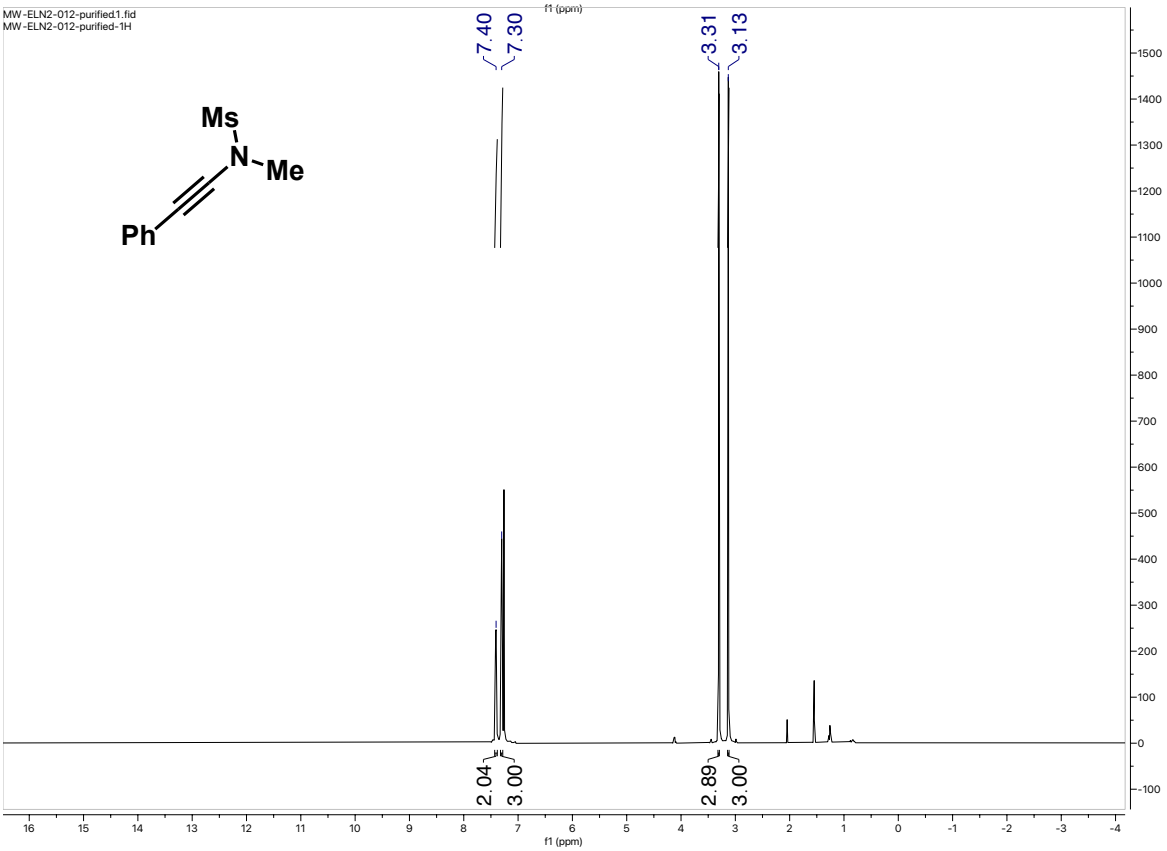

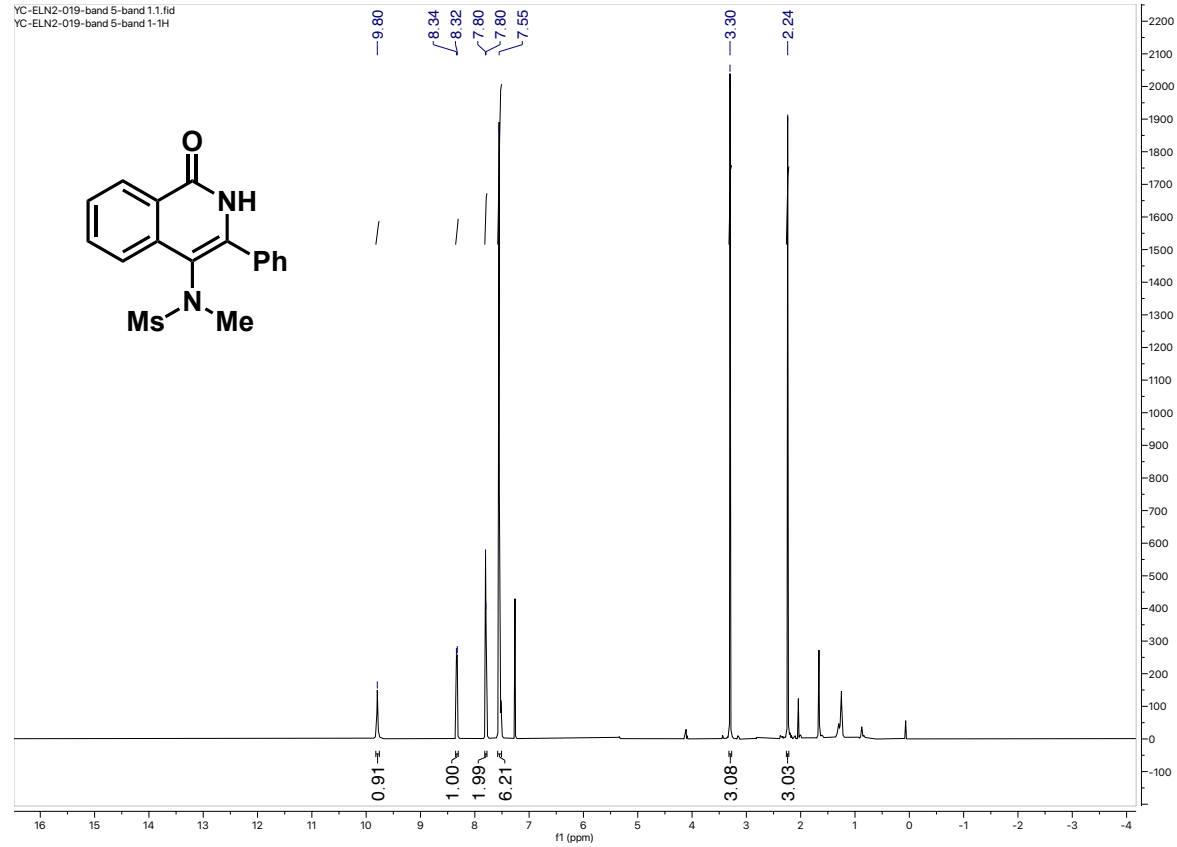
YC-ELN2-019-band 5-band 1.1.fid
YC-ELN2-019-band 5-band 1-1H
9.80
8.34
8.32
7.80
7.80
7.55
3.30
2.24
O
NH
Ph
N
Ms
Me
0.91
1.00
1.99
6.21
3.08
3.03
f1 (ppm)

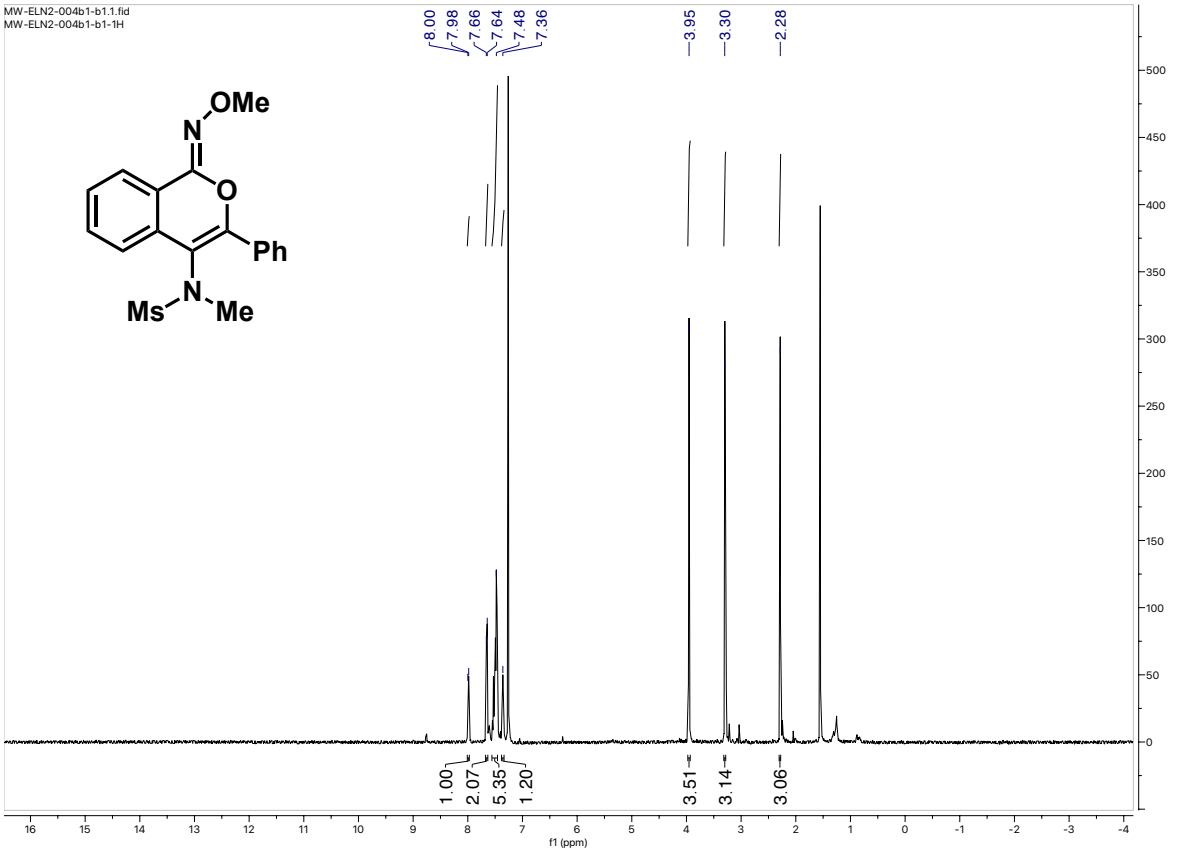
MW-ELN2-004b1-b1.1.fid
MW-ELN2-004b1-b1-1H
8.00
7.98
7.66
7.64
7.48
7.36
3.95
3.30
2.28
OMe
N
O
Ph
N
Ms
Me
1.00
2.07
5.35
1.20
3.51
3.14
3.06
f1 (ppm)

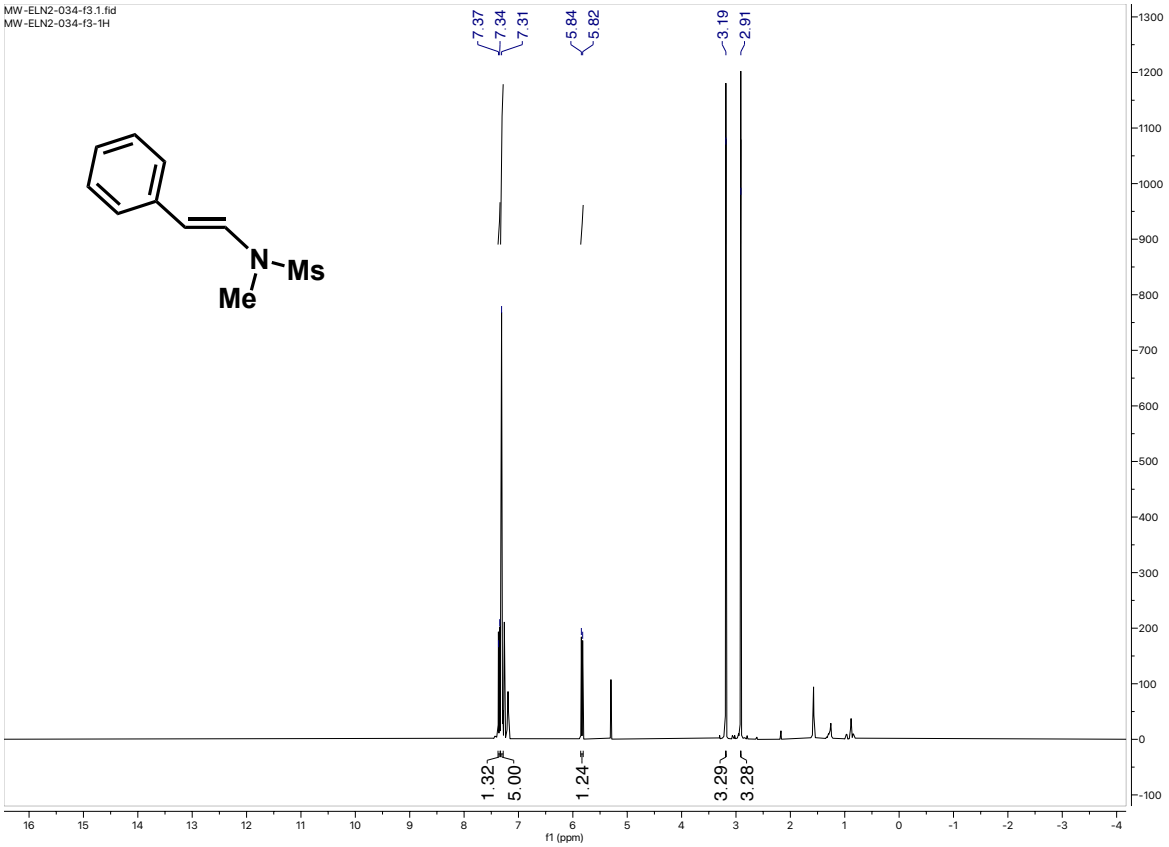
MW-ELN2-034-f3.1.fid
MW-ELN2-034-f3-1H
7.37
7.34
7.31
5.84
5.82
3.19
2.91
N
Ms
Me
1.32
5.00
1.24
3.29
3.28
f1 (ppm)

REFERENCES

Banjare, Shyam Kumar, et al. "*O*-Directed C–H Functionalization *via* Cobaltacycles: A Sustainable Approach for C–C and C–Heteroatom Bond Formations." *Chemical Communications*, vol. 57, no. 30, 4 Mar. 2021, pp. 3630–3647, https://doi.org/10.1039/d0cc08199j.

Beck, Hartmut, et al. "Small Molecules and Their Impact in Drug Discovery: A Perspective on the Occasion of the 125th Anniversary of the Bayer Chemical Research Laboratory." *Drug Discovery Today*, vol. 27, no. 6, June 2022, pp. 1560–1574, https://doi.org/10.1016/j.drudis.2022.02.015.

Brik, Ashraf, et al. "Rapid Diversity-Oriented Synthesis in Microtiter Plates for in Situ Screening of HIV Protease Inhibitors." *ChemBioChem*, vol. 4, no. 11, 3 Nov. 2003, pp. 1246–1248, https://doi.org/10.1002/cbic.200300724.

Colby, Denise A., et al. "Rhodium-Catalyzed C−C Bond Formation via Heteroatom-Directed C−H Bond Activation." *Chemical Reviews*, vol. 110, no. 2, 13 Feb. 2009, pp. 624–655, https://doi.org/10.1021/cr900005n.

Daley, Sharna-kay, and Geoffrey A. Cordell. "Alkaloids in Contemporary Drug Discovery to Meet Global Disease Needs." *Molecules*, vol. 26, no. 13, 22 June 2021, p. 3800, https://doi.org/10.3390/molecules26133800.

Guimond, Nicolas, et al. "Rhodium(III)-Catalyzed Isoquinolone Synthesis: The N−O Bond as a Handle for C−N Bond Formation and Catalyst Turnover." *Journal of the American*

Chemical Society, vol. 132, no. 20, 30 Apr. 2010, pp. 6908–6909, https://doi.org/10.1021/ja102571b.

Hara, Yusuke, et al. "Catalytic Formation of α-Aryl Ketones by C–H Functionalization with Cyclic Alkenyl Carbonates and One-Pot Synthesis of Isocoumarins." *Organic Letters*, vol. 17, no. 19, 17 Oct. 2015, pp. 4850–4853, https://doi.org/10.1021/acs.orglett.5b02414.

Heinrich, Michael, et al. "Alkaloids Used as Medicines: Structural Phytochemistry Meets Biodiversity—an Update and Forward Look." *Molecules*, vol. 26, no. 7, 25 Mar. 2021, p. 1836, https://doi.org/10.3390/molecules26071836.

Hou, Jingli, et al. "The Impact of Click Chemistry in Medicinal Chemistry." *Expert Opinion on Drug Discovery*, vol. 7, no. 6, 19 June 2012, pp. 489–501, https://doi.org/10.1517/17460441.2012.682725.

Huang, Yin-Hui, and Lin Dong. "Synthesis of Complex Dihydroisoquinolin Derivatives *via* Cobalt-electrocatalyzed C−H Activation." *Advanced Synthesis & Catalysis*, vol. 365, no. 1, 4 Jan. 2023, pp. 23–30, https://doi.org/10.1002/adsc.202201155.

Kolb, Hartmuth C, and K.Barry Sharpless. "The Growing Impact of Click Chemistry on Drug Discovery." *Drug Discovery Today*, vol. 8, no. 24, 15 Dec. 2003, pp. 1128–1137, https://doi.org/10.1016/s1359-6446(03)02933-7.

Kou, Xuezhen, and Kevin G. Kou. "A-Arylation of Silyl Enol Ethers via Rhodium(Iii)-Catalyzed C–H Functionalization." *ACS Catalysis*, vol. 10, no. 5, 4 Feb. 2020, pp. 3103–3109, https://doi.org/10.1021/acscatal.9b05622.

Kurek, Joanna. “Introductory Chapter: Alkaloids - Their Importance in Nature and for Human Life.” *Alkaloids - Their Importance in Nature and Human Life*, 13 Nov. 2019, https://doi.org/10.5772/intechopen.85400.

Li, Xiao-Cai, et al. “Cp*-Free Cobalt-Catalyzed C–H Activation/Annulations by Traceless *n*,*o*-Bidentate Directing Group: Access to Isoquinolines.” *Organic Letters*, vol. 21, no. 8, 29 Mar. 2019, pp. 2863–2866, https://doi.org/10.1021/acs.orglett.9b00866.

Niu, Ben, et al. “Catalyst-Controlled Synthesis of 4-Amino-Isoquinolin-1(2*h*)-One and Oxazole Derivatives.” *Organic Chemistry Frontiers*, vol. 5, no. 9, 8 Mar. 2018, pp. 1466–1470, https://doi.org/10.1039/c8qo00125a.

Vitaku, Edon, et al. “Analysis of the Structural Diversity, Substitution Patterns, and Frequency of Nitrogen Heterocycles among U.S. FDA Approved Pharmaceuticals.” *Journal of Medicinal Chemistry*, vol. 57, no. 24, 7 Dec. 2014, pp. 10257–10274, https://doi.org/10.1021/jm501100b.

Wang, Fen, et al. “Co(III)-Catalyzed Synthesis of Quinazolines via C–H Activation of *n*-Sulfinylimines and Benzimidates.” *Organic Letters*, vol. 18, no. 6, 8 Mar. 2016, pp. 1306–1309, https://doi.org/10.1021/acs.orglett.6b00227.

Webb, Nicola J., et al. “Rhodium(III)-Catalyzed C–H Activation/Annulation with Vinyl Esters as an Acetylene Equivalent.” *Organic Letters*, vol. 16, no. 18, 28 Sept. 2014, pp. 4718–4721, https://doi.org/10.1021/ol502095z.

Wu, Jia-Qiang, et al. “Experimental and Theoretical Studies on Rhodium-Catalyzed Coupling of Benzamides with 2,2-Difluorovinyl Tosylate: Diverse Synthesis of Fluorinated Heterocycles.” *Journal of the American Chemical Society*, vol. 139, no. 9, 23 Mar. 2017, pp. 3537–3545, https://doi.org/10.1021/jacs.7b00118.